



Universiteit  
Leiden  
The Netherlands

## Quantifying nucleosome dynamics and protein binding with PIE-FCCS and spFRET

Martens, C.L.G.

### Citation

Martens, C. L. G. (2023, February 1). *Quantifying nucleosome dynamics and protein binding with PIE-FCCS and spFRET*. *Casimir PhD Series*. Retrieved from <https://hdl.handle.net/1887/3514600>

Version: Publisher's Version

License: [Licence agreement concerning inclusion of doctoral thesis in the Institutional Repository of the University of Leiden](#)

Downloaded from: <https://hdl.handle.net/1887/3514600>

**Note:** To cite this publication please use the final published version (if applicable).

---

## QUANTIFYING TRANSCRIPTION FACTOR AFFINITY IN CHROMATIN

---

*Transcription factors (TFs) are proteins that bind to specific binding sites or recognition sequences in the promotor region of genes and are essential in the transcription regulation. Binding sites are often located at the DNA exits of the nucleosome; unwrapping nucleosomes from their ends, facilitates access of transcription factors to the nucleosomal DNA. To gain a mechanistic insight into the function of TFs and its interaction with chromatin, it is relevant to study its interactions with techniques capable of resolving the appropriate time scales under physiologically relevant conditions.*

*We combined Fluorescence Cross-Correlation Spectroscopy (FCCS) with Pulsed Interleaved Excitation (PIE) to quantify the binding affinity of the Glucocorticoid Receptor (GR) in the ex vivo environment of a nuclear extract to mimic in vivo molecular crowding as well as competition and cooperativity from other proteins and pioneering factors. We have shown previously that a Glucocorticoid Response Element (GRE) embedded in the Widom 601 nucleosome increased the opening and closing rates. We performed our measurements in nuclear extract to relate breathing dynamics to binding affinity in a single experiment; we observed that in the nuclear extract environment, the affinity of GR was most affected by DNA compaction, concurring with previous research in vitro, and less by the position of the GRE in the nucleosomes. In addition, we used FCS to quantify the specificity of the c-Jun protein, another transcription factor, for DNA containing or lacking its recognition sequence and found that the protein is capable of condensing both DNA constructs regardless of a recognition site present. The ex vivo experiments on GR bridge the observations made in vivo and in vitro by showing how a proteins' binding affinity and specificity are related to binding sites in compacted DNA in the presence of an abundance of unknown proteins, while keeping track of the relevant constituents in the environment.*

This chapter is in collaboration with:

M. van Eikenhorst, S. Grevink, D. Zandstra, M. Schaaf, Leiden University.

---

## 6.1 Introduction

Transcription factors (TFs) are proteins that bind to specific binding sites or recognition sequences in the promotor region of genes[231]. These proteins play a pivotal role in the transcription regulation. *In vivo*, transcription factors interact with not only with DNA but also with a host of other proteins that organize DNA[232][233]. Protein interactions with DNA condensed into chromatin have been shown to occur with association and dissociation times on a wide timescale (microseconds to minutes)[234][95][50] and with an affinity that is influenced by DNA sequence[233].

Transcription factor binding to DNA is expressed in affinity as well as specificity (or the inverse: promiscuity)[235][236]. Binding (or absolute) affinity is the ratio between the concentrations of free protein, DNA containing binding site, and their complex in molar dimensions ( $K_d$  [ $M$ ]) whereas specificity involves both binding to a specific partner and not binding to other proteins or binding sites ( $K_d^{absolute}/K_d^{general}$ ), and is often used to qualitatively describe protein interactions [237][236]. Specificity has also been described as local affinity, depending on possible interactions between a protein and binding site in close proximity of the target site, i.e. on the concentrations of all proteins and binding sites present locally[238]. Local differences in concentrations occur *in vivo* through several mechanisms (compartmentalization, phase separation), as opposed to *in vitro*, where concentrations of the constituents are expected to be homogeneous. Also, *in vitro* all constituents (proteins, binding sites, buffer composition) are known, making it in principle possible to calculate the affinities of all interactions. Because of these different environments, different measuring techniques and environments are often used, making an absolute parameter such as affinity, difficult to compare[239].

A transcription factor for which a wide range of affinities was found is c-Jun[240]. As either a homodimer, or a heterodimer with a closely related protein[241], it forms AP-1 (activation factor 1) [242], which is involved in transcription initiation [243][244]. Depending on being a monomer or a dimer, reported affinities of c-Jun for its specific DNA binding sequence (TRE: TPA responsive element) ranged from 10-12 nM (c-Jun/c-Fos, methylated and unmethylated DNA) [245] [246] to between 30 nM and 100 nM (c-Jun dimer, recombinant) [247][248][249] *in vitro*. Binding to non-specific sequences resulted in affinities as low as 2147 nM [246]. It was also observed that without the presence of closely related protein c-Fos, affinity

for DNA decreased [250][251] and c-Jun dissociated within seconds from DNA[252]. *In vivo*, similar trends were observed in ChIP-Seq experiments; however, as c-Jun associates with a multitude of proteins[253][254][255], these results are often difficult to interpret[256][257].

The Glucocorticoid Receptor (GR) is in many ways similar to c-Jun; after activation by a steroid hormone[258], it too can form homo- as well as heterodimers [259][260], which interact either directly with DNA or through tethering with a multitude of other proteins[261][262] and has been ascribed a pioneering role in transcription[263][264]. The binding affinity of GR for DNA depends on the conservation of, as well as the position of the recognition sequence (GRE)[94][95]. Affinity also increased when DNA was compacted in nucleosomes[91][92].

Another thing c-Jun and GR (and many other proteins) unfortunately have in common is the difficulty to relate their behavior *in vitro* to *in vivo*. A variation of dissociation constants of GR for nucleosomal DNA with GRE at different locations in the nucleosome were reported from *in vitro* and *ex vivo* measurements [91][93][95]; however, the experimental methods were based on fixed complexes (ELISA, gel-shift assays, single-color TIRFM) or lacked the complex environment that is found *in vivo* by using recombinant or purified proteins. On the other hand, *in vivo* measurements have characterized interactions ranging from milliseconds up to minutes[85][234][265], but lack the positional accuracy[50][266].

In order to bridge the gap between well-controlled *in vitro* experiments and *in vivo* measurements in bulk, here we combine pulsed interleaved interaction (PIE) with fluorescence cross-correlation spectroscopy (FCCS) for *ex vivo* to characterize the interaction of c-Jun with DNA containing and lacking the TRE sequence, and to quantify the affinity of GR in nuclear extract to the Widom 601 sequence. In this DNA sequence, the GRE was embedded at different positions so that, when the DNA constructs were condensed into nucleosomes, the GREs were positioned in one of the nucleosomal exits.

---

## 6.2 Materials and methods

### 6.2.1 DNA containing c-Jun and GR response elements

The response element for c-Jun, 5'-TGA<sup>CT</sup>CAG-3', was inserted into a DNA construct with an ATTO647N modified primer via PCR. The size of the DNA construct was 198 base pairs and contained the Widom 601 sequence between base pairs 40 and 191. The c-Jun part of the GJE sequence was positioned at base pairs 53 to 60. The Widom 601 sequence itself included several partial c-Jun response elements, most notably 5'-TCAG-3', at different locations. DNA-GJE also contained a GR response element.

Several DNA constructs were made containing the complete Glucocorticoid Response Element (GRE) 5'-TCTTGTtgcACAAGA-3' or half the element: 5'-TCTTGTtgcctcagc-3' (hGRE). The GRE was inserted through a modified primer at the PCR step (see Supplement for primers, protocols, DNA sequences and label positions). The DNA constructs were labeled with ATTO647N at base pair 41. DNA was mixed with human recombinant histones in a titration of molar ratios ranging from 1:1 to 1:3. Nucleosomes were reconstituted by salt gradient dialysis from 2 M to 0 mM NaCl overnight. Only titrations where no unreconstituted DNA was detected in gel after electrophoresis were used for F(C)CS experiments. Measurement buffers contained 10 mM Tris and 1 mM NaCl, unless stated otherwise. Nucleosome concentrations in FCS measurements were between 3 and 7 nM. Samples of 20 to 40  $\mu$ l were placed in a closed flowcell to minimize evaporation.

### 6.2.2 Recombinant c-Jun

Recombinant c-Jun was acquired from Active Motif (5  $\mu$ g, catalog no. 31116) diluted in buffer of 20 mM Tris-Cl (pH 8), 20% glycerol, 100 mM KCl, 1 mM DTT and 0.2 mM EDTA. The buffer used to perform FCS measurements consisted of 10 mM Tris-HCl (pH 8). The concentration of DNA was 2 nM in all measurements, c-Jun was added to obtain molar ratios 1:0.1, 1:0.3, 1:0.7 and 1:1 (DNA:protein).

### 6.2.3 GR transfection and activation

Human GR $\alpha$  N-terminally tagged with EYFP was obtained from transgenic COS-1 cells. As these cells are known to not express GR, complete labelling

of the GR population could be ensured.

COS-1 cells were grown in Dulbecco's Modified Eagle Medium (DMEM, Sigma D1145) containing 4500 mg/L glucose before transfection. DMEM lacked L-glutamine, sodium pyruvate and phenol red; therefore glutaMAX-1 (2 mM) and sodium pyruvate (1 mM) were added to the DMEM stock. Phenol red was omitted to minimize background of red fluorescence during FCS measurements. Fetal calf serum (fcs) was 10x diluted in the incubation buffer. Cells were grown at 37°C and 5% CO<sub>2</sub>. Cell transfer was performed after 3-4 days with trypsin added as a mixture of 45 ml/L PBS/EDTA plus 5 mL 10x trypsin 25%. Cells were transferred into T25 vials at 1 to 10 ratio. COS-1 cells were transfected with a GR-EYFP DNA vector provided by dr. Schaaf[267]. Our transfection protocol was based on a protocol from Fugene HD transfection reagent (Promega). At 80% confluency cells were detached from the T25 vial into 2 mL DMEM $\Delta$ fcs. Cells were plated on p-100 plates at a density of  $7.5 \cdot 10^5$  cells per plate. DMEM $\Delta$ fcs was added to an end volume of 4 mL per plate and incubated at 37°C for 24 hours. 10  $\mu$ g of the plasmid containing EYFP-hGR was dissolved in 1 mL DMEM $\Delta$ fcs plus 30  $\mu$ L Fugene HD (left for 2 hours at room temperature prior to incubation). The cells were incubated at 37°C for 24 hours after which the medium was refreshed with DMEM $\Delta$ fcs and incubated for another 24 hours. After this, the percentage of transfected cells was determined using a confocal microscope (EVOS FLAuto2, Thermofisher). This percentage was between 70% and 85% (N = 4).

hGR-EYFP was activated with corticosterone or dexamethasone in EtOH. 30  $\mu$ L of 1 mM of the hormone was added to the total volume of 30 mL and the cells were incubated for 50 minutes at 37°C.

Cytoplasmic and nuclear extracts were acquired following the protocol of the Nuclear Extract Kit (Active Motif, 40010/40410, protocol version D3). The cells were collected on ice in a PBS/Phosphatase Inhibitor buffer from the kit to minimize protein activity. The cells were then resuspended in Hypotonic Buffer from the kit to swell them and weaken their membranes. Detergent buffer was added to induce leakage of the cytoplasmic proteins into the supernatant. The samples were centrifuged for 30 seconds at 14000 x g in a micro-centrifuge cooled to 4°C. After collection of the supernatant containing the cytoplasmic fraction, the nuclei in the pellet were lysated and solubilized in Lysis buffer from the kit.

The extracts contained a plethora of other unlabeled proteins and the

---

overall protein concentration needed to be determined first. This was done by Bradford method (Coomassie Protein Assay Kit 23200, Thermoscientific). The total protein concentration in the nuclear extract containing GR activated with dexamethasone was 726  $\mu\text{g}/\text{mL}$ . A TransAM GR kit based on the ELISA method (Active Motif, 45496, protocol version A1) was used to determine GR activity in the cytoplasmic and nuclear extracts. The extracts were each loaded into a well of a 96-well plate coated with DNA oligomers containing the GRE consensus sequence (5'-GGTACAnnnTGTCT-3'). The TransAM protocol allows for 2-20  $\mu\text{g}$  of protein per well, so 5  $\mu\text{L}$  (= 3.6  $\mu\text{g}$ ) of the nuclear extract used in the Bradford was used for TransAM. The GR concentrations of all extracts were determined from FCS experiments, by assessing the number of proteins from the amplitude of the correlation curve and the average intensity (photons/sec). Extracts were diluted to match the EYFP-GR concentration of the dexamethasone-activated nuclear extract. By doing so, the relative difference in activity between extracts was measured.

After incubation of the GR in the extracts in the TransAM plate and washing, primary GR antibodies were added to the wells. After incubation and washing, secondary antibodies (anti-IgG HRP-conjugated) were added which were activated with a developing solution from the kit and stopped after 20 minutes. Directly after stop solution from the kit was added, absorbance was measured on a spectrophotometer at 514 nm using a reference absorbance at 655 nm.

#### **6.2.4 Single-molecule fluorescence correlation spectroscopy**

Measurements were performed on a home-built confocal microscope with a water-immersion objective (60x, NA 1.2, Olympus), using an ICHROME MLE-SFG laser. The excitation beam was directed via fiber coupler and a dichroic mirror (z514/640rpc, Chroma) into the objective and focused 50  $\mu\text{m}$  above the glass-sample interface. cJun-DNA measurements were done by continuous excitation at 632 nm. F(C)CS was performed on GR-DNA and GR-nucleosome in experiments using pulsed interleaved excitation (PIE) mode by alternating 514 nm (30  $\mu\text{W}$ ) and 632 nm (20  $\mu\text{W}$ ) 100 ns excitation pulses with 300 ns intermittent dark periods. Fluorescence was spatially filtered with a 50  $\mu\text{m}$  pinhole in the image plane and split by a second dichroic mirror (640dcxr, Chroma). The fluorescent signals were further filtered (hq570/100nm and hq700/75nm, resp.) and focused on the

active area of single photon avalanche photodiodes (SPADs, SPCM AQR-14, Perkin Elmer). The photodiodes were read out with a TimeHarp 200 photon counting board (Picoquant), and the arrival times of the collected photons were stored in t3r (time-tagged to time-resolved) files. PIE-F(C)CS measurements were done for a least 30 minutes, in recordings of at least 2 minutes. These recordings were further processed by home-built Python analysis programs.

### 6.2.5 FCCS analysis and binding affinity

Due to Brownian motion, fluorescently labeled molecules diffuse in and out of the confocal volume, causing the fluorescence intensity to fluctuate in time. The fluctuations of the intensity were analyzed by correlating the photon arrival times over increasing time-lag  $\tau$ :

$$G(\tau)_{diff} = \frac{\langle \delta I_1(t) \cdot \delta I_2(t + \tau) \rangle}{\langle I_1(t) \rangle \langle I_2(t) \rangle} \quad (6.1)$$

To assess the diffusion of a molecule photon streams  $I_1$  and  $I_2$  were correlated to generate an autocorrelation curve ( $I_1 = I_2$ ). To quantify the fraction of two differently labeled molecules diffusing through the focus at the same time (i.e. as a complex) the signal of one molecule ( $I_1$ ) was correlated with the signal of another molecule ( $I_2$ ) to generate a crosscorrelation curve. The correlation curve  $G(\tau)$  depends on the concentration and diffusion time of the labeled molecules, as well as the confocal volume which they diffuse through:

$$G(\tau) = N^{-1} \cdot (1 + \tau/\tau_D)^{-1} \cdot (1 + a^{-2} \cdot \tau/\tau_D)^{-1/2} \quad (6.2)$$

with diffusion time  $\tau_D$  and average number of molecules  $N$  in the focal volume. Parameter  $a$  is the ratio between the axial and radial size of the confocal volume and was determined through calibration experiments to be 8. Background signal, photophysics of the fluorophore (transiting to the triplet state / dark state) and afterpulsing effects were included in the fit of the correlation curve, see chapter 2 of this thesis. Binding affinity of proteins to DNA or nucleosomes was defined as the dissociation constant derived from the concentrations of proteins and DNA (or nucleosomes), and complex:



---

$$K_d = \frac{[DNA] \cdot [protein]}{[complex]} \quad (6.3)$$

The dissociation constant equals the concentration of DNA or nucleosome at which half of the available binding sites are occupied by protein. A lower value of  $K_d$  therefore corresponds to a higher affinity of the protein to the ligand.

## 6.3 Results

### 6.3.1 c-Jun interactions with DNA

Transcription factor c-Jun was added to DNA containing or lacking the response element GJE. Figures 5.1 a-d show representative time traces of different molecular ratios of c-Jun to DNA (all containing the GJE except fig. 6.1c). By qualitative observation it was obvious that increasing the c-Jun concentration introduced large DNA condensates. In order to quantify this, the mean and standard deviation (sd) of the intensity of fluorophore ATTO647N were calculated. In the absence of c-Jun, the photon signal of labeled DNA stayed almost completely within 2 sd of the average signal (figure 6.1a,  $I = 2.48 \pm 0.12$  kHz (mean  $\pm$  sd)). Upon introducing a 1:0.1 DNA to c-Jun ratio, the photon signal became more erratic and the standard deviation increased (figure 6.1b). Nevertheless, the photon signal was mostly within 2x sd (17% of the mean). At a DNA:c-Jun ratio of 1:0.3 (figure 6.1c) the effect of condensation was clearly visible. When measured for a longer time, parts of the time trace containing condensates could be discarded before for correlation analysis. However, measuring for 200 seconds did not yield enough data without condensates for the experiment 1:0.3 DNA(-):c-Jun to be used for correlation analysis.

At a 1:0.7 ratio of DNA:c-Jun time traces of both DNA(-) and DNA(GJE) contained very large condensates. As a result, the mean and sd were larger than we anticipated for the concentration of DNA. Next to very large aggregates, we also observed smaller condensates that could not fully be excluded from time traces, as shown in the inset of figure 6.1d.

Figure 6.1e shows the effectiveness of aggregate exclusion by selection. for DNA only, 1:0.1 and 1:0.3 DNA:c-Jun measurements the normalized curves overlapped. Correlation curves from 1:0.7 experiments resulted in a slightly worse fit (figure 6.1f).

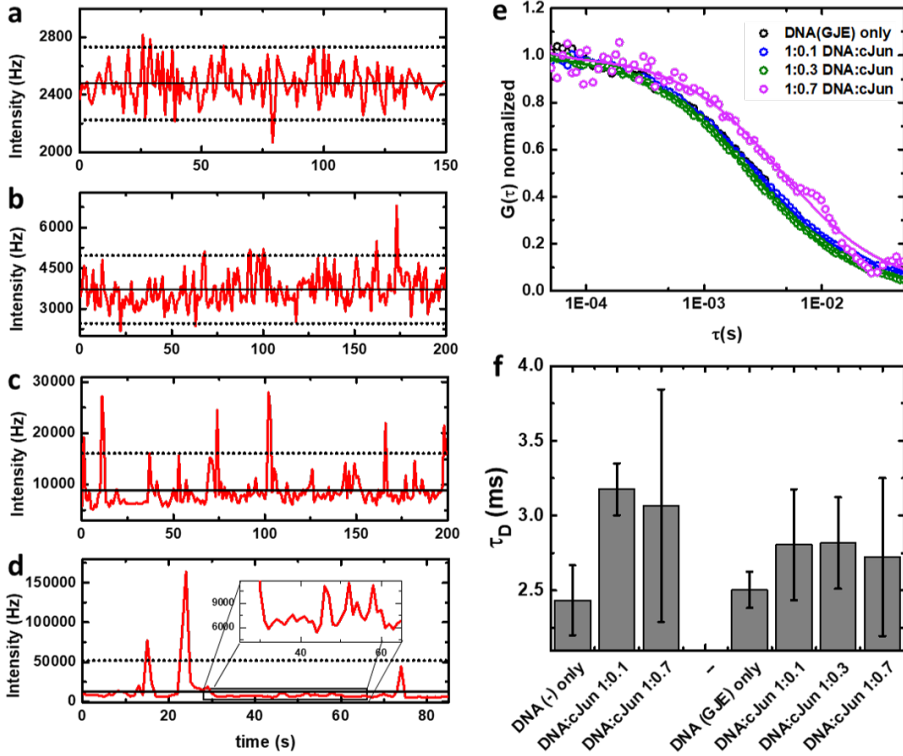


FIGURE 6.1: **Nonspecific aggregation of c-Jun on DNA.** **a) - d)** Time traces (red) of DNA(GJE)-ATTO647N from continuous 632 nm excitation, with no **(a)**, 1:0.1 **(b)**, 1:0.3 **(c)** and 1:0.7 **(d)** ratio of DNA to c-Jun. Increasing c-Jun concentration introduced more and large condensates, thereby increasing the variance (dots, 2x variance) from the intensity (mean = black line). **e)** Addition of unlabeled c-Jun to DNA resulted in correlation curves more difficult to fit with one population (purple curve). **f)** Averaging over several experiments and excluding aggregates yielded uncompromised correlation curves, with small deviations of the diffusion times, when bursts from condensates were discarded.

### 6.3.2 GR activity

In order to have a completely labeled population of a transcription factor, a DNA vector translating to GR fused to EYFP was used to transfect COS1 cells as described in the Methods section. After sufficient expression, GR was activated with dexamethasone or corticosterone. Figures 6.2a-f show

---

the localization of GR in the nucleus upon activation with dexamethasone. Directly after adding hormone, GR was predominantly localized in the cytoplasm; the nuclei are less fluorescent than the cytoplasm in figure 6.2a. After 24 minutes the cells' nuclei started to become brighter (figure 6.2c), and after 44 minutes GR appeared to be mostly localized in the nuclei. From previous activation experiments we learned to allow for 5 to 10 more minutes for residual GR to go into the nucleus (figure 6.1f).

After activation, cells were collected and lysated to obtain cytoplasmic and nuclear extract (described in Methods). GR concentration was determined through FCS measurements and average fluorescent intensities. Different extracts were diluted to similar concentrations to determine GR activity. The ELISA based TransAM kit was used as described. Figure 6.2g shows the optical density (OD, or extinction coefficient) at 514 nm excitation. The OD values of different samples revealed the relative GR activity. We observed that at similar concentrations, GR in nuclear extract activated with dexamethasone contained twice more functional GR compared to its cytoplasmic counterpart. This implies that half of the GR in the cytoplasmic extract could not bind to DNA and was therefore inactive. Cytoplasmic and nuclear extracts after corticosterone activation showed equal levels of GR activity, implying that the cytoplasm still contained a substantial population of activated GR. Subsequent experiments were performed with nuclear extracts after dexamethasone activation.

GR affinity for one of the DNA-GRE constructs (GRE3) was tested by EMSA. Figure 6.3a shows that GR in nuclear extract did not appear to have a defined band in the gel; the fluorescent signal in lane 1 showed a wide dispersion. Without nuclear extract the DNA appeared as a clear band (lane 2), when GR was added at a 1:1 ratio the signal of DNA was completely dispersed in the gel (lane #4). For higher concentrations of DNA the DNA signal became visible again, although not in a defined band (lanes 5-8 show ratios 1:2, 1:4, 1:8, 1:16 respectively); the signal of GR was still very dispersed in the lanes. We argue that unlabeled components (proteins, RNA) from the nuclear extract may interact nonspecifically with the GR and DNA, thereby preventing the formation or detection of clearly defined GR · DNA complexes.

Measuring GR in FCS was done in two modes of excitation: pulsed (PIE) and continuous (figure 6.3b). PIE reduced the photophysical effect known as flickering (blinking of fluorophore EYFP in the range of micro- to

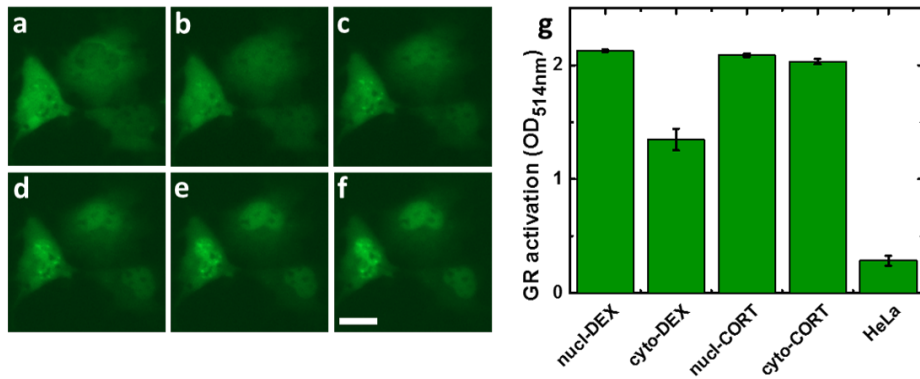


FIGURE 6.2: **Activated GR in nuclear extract binds to DNA containing a GRE.** a) - f) GR-EYFP in COS-1 cells was localized predominantly in the cytoplasm before activation. After activation with dexamethasone images were taken at 4 (a), 13 (b), 24 (c), 35 (d), 44 (e) and 50 minutes (f). Scale bar: 10  $\mu$ m. g) GR activity was measured with ELISA based method TransAM. GR activated with corticosterone mainly localized to the nucleus (nucl-CORT), but part of the active GR was still present in the cytoplasm (cyto-CORT). To estimate background, samples containing GR were compared to samples from HeLa cells (containing no EYFP labeled GR). Error bars represent standard deviations of 2 or more samples.

milliseconds) making the diffusion part of the autocorrelation curve more prominent. The resulting diffusion time of GR was  $3.6 \pm 0.7$  ms, which corresponds to a hydrodynamic radius of  $25 \pm 5$  nm. Considering the size of a GR dimer from electron microscopy studies to be in the order of 8 nm [268][187], the results from gel and PIE-FCS suggest that activated GR exists in a larger complex in the nuclear extract, even when taking into account the added size of the EYFP.

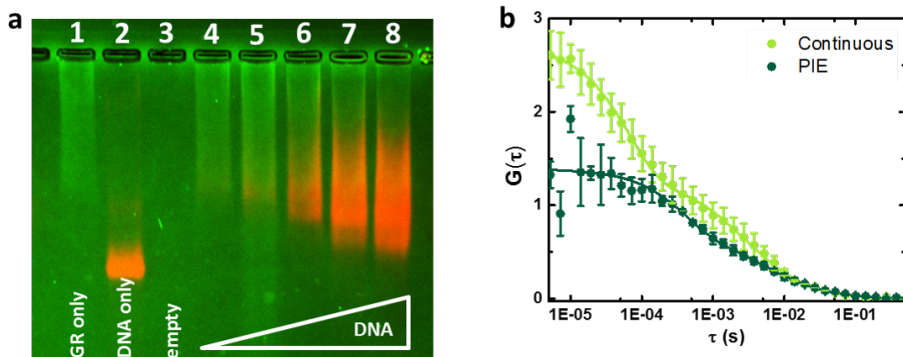


FIGURE 6.3: **Nuclear extract containing activated GR interacts nonspecifically with DNA.** **a)** Nuclear extract containing activated GR (EYFP labeled, green, lane 1) interacted with DNA construct GRE3 (Atto647N labeled, red, lane 2) in a 1% agarose gel. Molecular ratios of GR to DNA in lanes 4-8 were 1:1, 1:2, 1:4, 1:8 and 1:16. Unlabeled components of the nuclear extract seemed to nonspecifically interact with GR, as in lanes 1 and 4-8 its signal was dispersed as well. **b)** FCS with sub-microsecond PIE modulation reduced flickering of EYFP compared to continuous excitation with 514 nm. Fitting the autocorrelation curve from PIE-FCS measurements resulted in a diffusion time of  $3.6 \pm 0.7$  ms for GR.

### 6.3.3 GR affinity for DNA and nucleosomes

PIE-FCCS measurements were performed on DNA constructs GREh, GRE2 and GRE3 and the nucleosomes reconstituted using these DNA substrates (see supplement for full sequences). Nuclear extract containing GR activated with dexamethasone was added to a molecular ratio between DNA or nucleosomes with GR of approximately 1:1. Auto- and crosscorrelation curves were computed to quantify protein affinity. Figure 6.4a shows representative plots of these curves. The curves were fitted to eq. 5.2 to obtain the number of molecules for each species. In figure 6.4b the number GR proteins, nucleosomes and complexes fitted from FCS experiments on three reconstituted nucleosomes are shown. We obtained similar results for all sequences. We did the same measurements on bare DNA substrates and obtained very similar concentrations (data not shown).

From the obtained concentrations we calculated the binding affinities; all affinities were larger than 15 nM. The dissociation constants of the DNA constructs in figure 6.4c were similar for all substrates (hGRE:  $25 \pm 8$  nM,

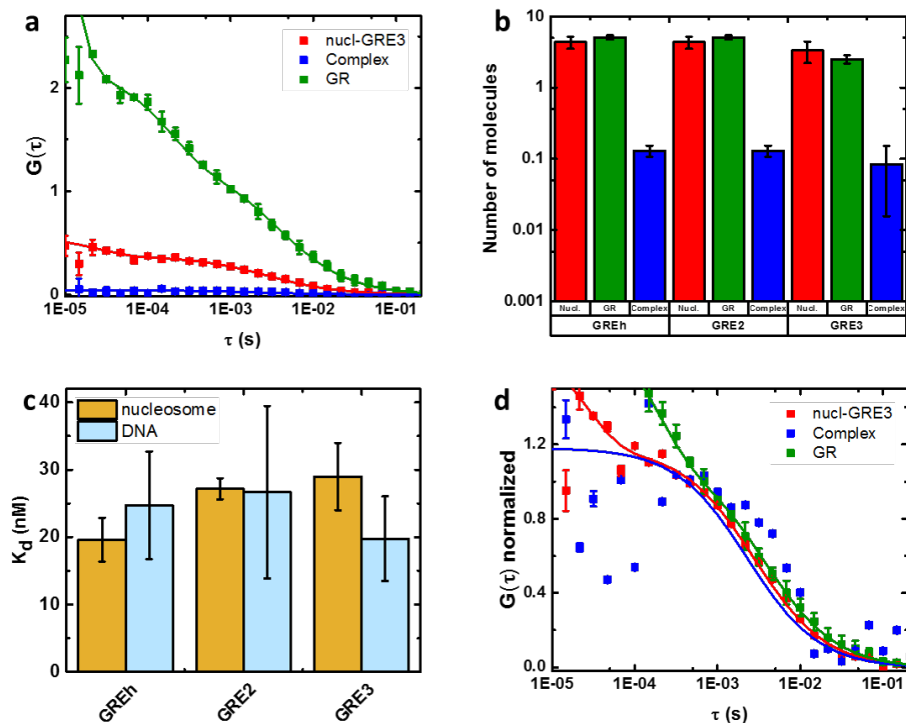


FIGURE 6.4: **GR-nucleosome binding depends on GRE position.** **a)** Representative auto- and crosscorrelation curves from photon signals corresponding to nucleosome (red), GR (green) and the complex nucleosome-GR (blue). **b)** The concentrations from fitting the correlation curves were used to calculate the dissociation constant  $K_d$  for three DNA constructs incorporating the GRE. **c)** Dissociation constant for nucleosome-GR interaction shows a trend of decreasing affinity when the GRE is positioned more towards the nucleosome dyad. Between DNA constructs where the position of the GRE differed no difference in affinity was observed. **d)** Normalization of the correlation curves in 5.4a shows that the complex is not diffusing significantly slower compared to either GR or nucleosome.

---

GRE2:  $27 \pm 13$  nM, GRE3:  $20 \pm 6$  nM). Nucleosome hGRE ( $K_d$ :  $20 \pm 3$  nM) appeared to have a slightly higher affinity than GRE2 ( $K_d$ :  $27 \pm 2$  nM) and as GRE3 ( $K_d$ :  $29 \pm 5$  nM). This result cannot confirm the GRE was less accessible to GR when placed further inside the nucleosome.

As the DNA-GR complex made up a very small part of the mix, the resulting crosscorrelation curves had a small amplitude. For better visualization the curves were normalized (figure 6.4d). Unexpectedly, the fit to the curve corresponding to the complex had a similar diffusion time as the free nucleosome, suggesting a more complex binding pattern. The diffusion times of the DNA/nucleosomes and GR in interaction experiments did not differ significantly compared to their diffusion times without the other component. However, because of increased noise, the crosscorrelation curve could not be fitted as accurately as one species of molecules.

### 6.3.4 Increasing nucleosome concentration increases complex concentration

Because the concentration of bound GR was close to the detection limit, we repeated the experiment at higher nucleosome concentrations. Indeed, the number of nucleosome-GR complexes increased and fits of both experiments resulted in similar dissociation constants:  $34 \pm 4$  nM (1:1) and  $25 \pm 4$  nM (1:10). Because the number of molecules were more difficult to fit for the complex (figure 6.4d), we decided to also investigate the changes in diffusion time of the nucleosome and GR in interaction experiments.

Upon increasing the concentration of nucleosomes, the correlation curves shifted to slightly larger correlation times (orange and red curve in figure 6.5b). However, fitting the correlation curves did not result in significantly different diffusion times (figure 6.5c, red bars). The same was found for the diffusion times of GR (figure 6.5c, green bars).

Summation of simulated correlation curves of nucleosomes consisting of free nucleosomes and nucleosomes bound to an increasing fraction of GR protein offered an explanation for the absence of differences seen in our experiments: the inset in figure 6.5d shows that the curves for 0% and 25% bound cannot be distinguished from one another, assuming a standard deviation of 5%. This implied a higher affinity (resulting in a higher percentage of bound protein) is needed in order to confirm binding through difference in diffusion times. Simulated data were computed by composing a  $\tau_D$  of different fractions of the diffusion times of free nu-

cleosomes and nucleosomes bound to GR; for the latter we assumed the diffusion times of nucleosome and GR as found in measurements, and in a 1:1 binding ratio. For example, for 25% binding, the diffusion time was calculated as  $\tau_{D,comp} = 0.75 \cdot \tau_{D,freeNucl} + 0.25 \cdot \tau_{D,boundNucl}$ , with  $\tau_{D,boundNucl} = \tau_{D,freeNucl} + \tau_{D,freeGR}$ .

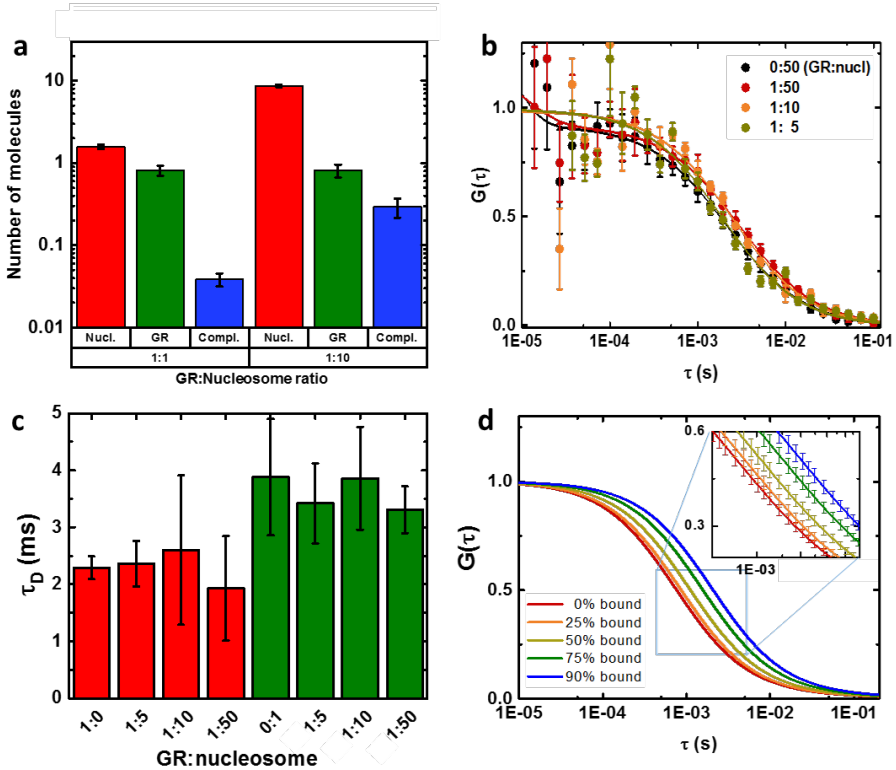


FIGURE 6.5: Increasing concentrations of GR or nucleosome increased concentration of the GR-nucleosome complex. **a**) Increasing nucleosome concentration tenfold increased the complex concentration. **b**) Increasing nucleosome GRE3 concentration showed a small shift for higher concentrations of nucleosome. **c**) However, diffusion times of nucleosome GRE3 or GR did not increase significantly upon increasing the concentration of nucleosome. **d**) Simulating nucleosome diffusion with increasing GR binding revealed a significant difference in correlation curve could only be observed when more than 25% bound protein.



---

## 6.4 Discussion and conclusions

Using FCS we demonstrated that mixing recombinant c-Jun with DNA constructs both lacking and containing a c-Jun binding element induces DNA aggregation. For both DNA constructs the size of the condensates increased with the concentration of c-Jun, while their frequency seemed to decrease. We did not quantify the frequency and intensity of the condensates, but FCS does offer the possibility to do so, since we were able to identify and exclude (most of) them from further analysis. We have shown that after exclusion of condensates, addition of c-Jun slightly increased the diffusion time of DNA. Increasing the concentration of c-Jun did not further increase the diffusion time of DNA when the signal was filtered from condensate contributions. These observations point to nonspecific interactions of c-Jun with DNA and might imply a DNA-condensing role for c-Jun during transcription. It is possible to increase specificity of c-Jun through methylation of the DNA binding site [245] [246] or addition of the protein c-Fos[250][251]; however, as we were not able to tag c-Jun with a fluorescent label, further experiments to see if c-Jun has a higher affinity for methylated DNA constructs containing the GJE binding element were not pursued.

For GR to exhibit any binding to DNA, the protein needs to be activated to detach from the heat shock proteins complex it resides in when in the cytoplasm[269]. We used dexamethasone as well as cortisol to activate GR. Translocation to the nucleus occurred for both hormones. As described, COS-1 cells containing activated GR were processed in both nuclear extracts and cytoplasmic extracts. All extracts were tested with an ELISA kit; the cytoplasmic extract from dexamethasone activation exhibited a lower affinity than the associated nuclear extract, implying a difference in activity. A difference in binding affinity depending on the hormone used for activation has been observed before by Schaaf et al.[258][234][265]

In agarose gel, GR-EYFP(dex) in the nuclear extract was visible as a smeared band in the high molecular weight region around 1000-1200 bp. The smearing might stem from nonspecific, short-lived interactions with other proteins in the extract[270][271][261] as has been observed before in gel for nucleosomes and purified GR by Perlmann et al. [91][93][92], and nucleosomes and LexA by Li and Widom[50]; it could also be an intrinsic property of the GR existing in a disordered state, which is often related to a protein's level of activity [272][273]. Adding a 200bp DNA construct labeled with Atto647N resulted in the DNA construct smearing in the lane centered around size 500

bp. Increasing the ratio of DNA to nuclear extract widened the DNA smear but shifted its center to smaller sizes. A possible explanation for this is that more DNA may distribute proteins in the extract over more DNA fragments, yielding less complexes carrying multiple DNA binding proteins, thus allowing DNA to move further down through the gel. The smearing appeared to be independent of a GRE present in the DNA construct, fortifying the idea that not only the GR, but also other proteins in the extract interacted with the DNA [264][263][262].

Consistent with this, in FCCS the cross-correlation curve, complexes of GR with either DNA or nucleosome, were barely visible, implying a low concentration of a complex. For all DNA and nucleosome constructs the binding affinities were 20 nM and larger. Statistically there was no significant difference in  $K_d$  for DNA constructs GREh, GRE2 and GRE3, which was different than previous results from Jin[95] and Wrangle[94][181], who have shown that the compaction of DNA into nucleosomes, as well as embedding the GRE position in nucleosomes increases the affinity of GR. Here, GR had the highest affinity for nucleosomes reconstituted from GREh DNA. Although differences in affinity were small, it appeared that  $K_d$  depends on accessibility of the GRE in nucleosome, i.e. having a GRE positioned closer to the nucleosomal exit increases access for GR. The difference in affinity of GR for GRE-nucleosomes might become more apparent though at higher salt concentrations, as we have shown in this thesis that differences in nucleosomal dynamics and stability appeared mostly at salt concentrations higher than 15 mM.

As mentioned, the signal in the cross-correlation channel was very low (10-100 photons/sec), requiring long data acquisition times. In addition, we observed anti-correlation at microsecond timescales, likely from EYFP photophysics[127]. Despite these technical difficulties, the small amplitude cross-correlation curve does show a plateau at larger tau (implying slower diffusion, i.e. larger molecule) compared to the autocorrelation curves from GR and DNA. The incline of the slope however, is steeper and uncharacteristic of normal 3D diffusion, implying more convoluted dynamics than only diffusion. The timescale of the steeper incline (milliseconds) does not coincide with that of EYFP-flickering, which happens at shorter times (nano to microseconds). Our curve-fitting algorithm converged most of the times to a plateau of the curve (fits were visually inspected after automated fitting), allowing for estimation of the complex concentration.

---

The binding affinities found via PIE-FCCS resembled those reported *in vitro* [92][181]. Observations in FCS and in gel matched nonspecific binding observed *in vivo* [234][233][274], where binding times of milliseconds are the predominant mode of interaction[265].

*In vivo*, specific binding events of seconds to minutes have been reported, which may be enhanced through crowding [275][276][277][278][279]. Physiological crowding conditions can be mimicked through adding PEG to DNA-GR mixtures; however, addition of PEG to nucleosomes causes the nucleosomes to aggregate, and slows the diffusion of all constituents in the sample, which would then needed to be characterized through separate measurements.

A small shift in the correlation curve of nucleosome GRE3 towards larger  $\tau$  was observed when increasing the ratio of nucleosome to GR, but the difference was so minute it did not lead to significantly larger diffusion times when fitted. This observation points again toward an abundance of nonspecific interactions of the constituents in the extract with DNA or nucleosomes.

During measurements, large condensates of both DNA/nucleosomes and GR were observed, but the frequency and intensity differed between extracts and were therefore initially discarded. It might be that these condensates are the *ansatz* of pre-complex bubbles, increasing local protein concentrations by macromolecular crowding / volume exclusion [280][281][282][283].